

Azo polymers for reversible optical storage: 13. Photoorientation of rigid side groups containing two azo bonds

X. Meng and A. Natansohn*

Department of Chemistry, Queen's University, Kingston, Ontario, Canada K7L 3N6

and P. Rochon

Department of Physics, Royal Military College, Kingston, Ontario, Canada K7K 5L0

(Received 13 June 1996)

Copolymers of methyl methacrylate with a methacrylate containing a rigid group with two azo bonds (3RM) were prepared and their photoinduced birefringence levels and rates studied. Birefringence levels of 0.11 for the copolymer with 11.6 mol% azo structural units and 0.13 for the copolymer with 30.0 mol% azo structural units were found; this is higher than the birefringence inducible in a typical azo homopolymer containing a chromophore with only one azo group, poly{4'-[(2-(acryloyloxy)ethyl)ethylamino]-4-nitroazobenzene} [poly(DR1A)]. The birefringence per azo structural unit for a copolymer containing 11.6 mol% 3RM is about five times that for a DR1A copolymer with similar azo content, because of the intrinsic structural properties of 3RM (high length/diameter ratio). Dichroism in both u.v. and visible regions of the spectrum contribute to the overall photoinduced birefringence. The rate of inducing birefringence in the 3RM copolymers is lower than in poly(DR1A) and the birefringence stability (91–96% of the induced birefringence is maintained after the writing laser is off) is much better than that for poly(DR1A) (about 80%). The good stability and slow birefringence growth rate are due to the lesser mobility of the larger side group. © 1997 Elsevier Science Ltd.

(Keywords: photoinduced birefringence relaxation; side groups with two azo bonds; kinetics of orientation)

INTRODUCTION

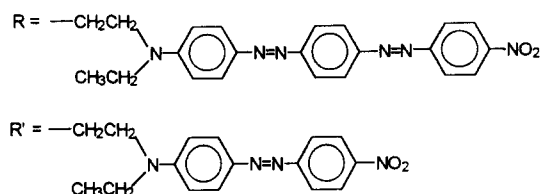
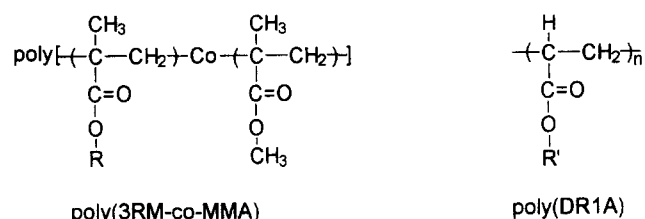
Polymers containing substituted azobenzene groups are being studied as optical storage materials¹. For 'writing', anisotropy can be induced by the orientation of azobenzene groups when exposing a polymer film to a linearly polarized laser. The mechanism is based on the selective excitation of the azobenzene groups having a dipole component parallel to light polarization. They undergo a multitude of *trans*–*cis*–*trans* isomerization cycles accompanied by reorientation, thus increasing the concentration of azobenzene groups perpendicular to the polarization direction. This mechanism involves extensive motion of the side groups and of the main chain of the polymer below its glass transition temperature (T_g). When an oriented spot in a polymer film is irradiated by a circularly polarized laser, or heated above T_g , the anisotropy will be 'erased' back to the random state of the 'unwritten' area^{2–4}.

Excited by a polarized laser, the *trans*–*cis* isomerization rate for an azobenzene molecule is proportional to the term $I \cdot \cos^2(\phi)$, where I is the laser beam intensity, and ϕ is the angle between the azobenzene axis and the laser polarization direction². When shining a linearly polarized laser on a polymer film, the azo groups which are not perpendicular to the laser polarization direction

will undergo many *trans*–*cis*–*trans* isomerization cycles accompanied by reorientation until they fall in one of the directions (in a plane) perpendicular to the laser polarization direction at the end of one of the *cis*–*trans* isomerizations. All the azo groups in that plane will conserve their orientation, because they cannot be photoreactivated when $\cos^2(\phi) = 0$. The net result is an orientation distribution with an excess of azo groups in the direction perpendicular to the laser polarization. This orientation can be detected as birefringence by another laser beam. Most of the azo groups will not reach the plane perpendicular to the laser polarization. They will keep isomerizing between *trans* and *cis* forms during the laser irradiation and some will relax to a random distribution after the laser beam is turned off. This is one of the reasons for birefringence relaxation. Circularly polarized light activates all azo groups in the plane of the film, thus it destroys the preferential orientation induced by the linearly polarized light.

The optical response of the polymer is mainly influenced by three structural factors: the polymer backbone, the structure of the azo chromophore and the linkage between the backbone and the azo chromophore. The type of polymer backbone mostly dictates the mechanical properties, such as the T_g of the polymer. The linkage between the azo chromophore and the polymer backbone affects both the mechanical properties and the motion of the azo groups, and thus their

* To whom correspondence should be addressed



Scheme 1

orientation. The structure of the azo chromophore determines properties such as the wavelength of maximum absorbance, the *cis*–*trans* thermal isomerization rate, the orientation ability, as well as the order parameter. In some previous studies in our laboratory^{5,6}, it was found that the rate of achieving birefringence and the level of induced birefringence depend on the type and the size of the azo groups.

The birefringence photoinduced by a linearly polarized laser at room temperature is produced mainly by the motion of the side chain groups. The rate of inducing birefringence can be described by a biexponential process where the fast process is usually associated with the side groups motion and the slow process is usually associated with the main chain motion^{5,6}. As we reported recently¹, the rate of birefringence growth for both of the fast motion and the slow motion decreases when the operating temperature increases because of the thermal randomizing of the oriented azo groups. The decrease is more significant for the side groups motion, thus one could in principle achieve a higher birefringence level by reducing the side chain mobility.

Among all azo-containing polymers reported in the literature, a polymer containing a rigid side group with two azo bonds between three benzene rings appears to be very interesting because it was found to have a larger order parameter⁷, and $\chi^{(3)}$ in comparison to polymers containing azobenzene groups in the side chain^{8–10}. A copolymer containing such a rigid group was also reported for potential second-order nonlinear optical applications¹¹. Such a polymer film can be subjected to polarized light to photoinduce orientation of the chromophore, but the mechanism has to be more complex than in the polymers containing substituted azobenzene. The photoinduced *trans*–*cis* and *cis*–*trans*, and the thermal *cis*–*trans* isomerizations will take place in both azo groups. Consequently, the alignment of the whole side group may take more time. On the other hand, the large conjugated structure in the chromophore with two azo groups may generate a larger birefringence per structural unit, because of the larger length/diameter ratio of the chromophore^{12–14}. We report here the behaviour of a polymethacrylate bearing a chromophore with two azo groups between three benzene rings.

poly{4-[[2-[(2-methyl-1-oxo-2-propenyl)oxy]ethyl]ethylamino]-4'-(4-nitrophenylazo)azobenzene-co-methyl methacrylate} [poly(3RM-co-MMA)]. Comparison is made with poly{4'-[(2-acryloyloxy)ethyl]ethylamino]-4-nitroazobenzene} [poly(DR1A)] bearing a substituted azobenzene side group. The structures of the two polymers are shown in Scheme 1.

EXPERIMENTAL

N-Ethyl-*N*-(2-hydroxyethyl) aniline and 4-amino-4'-nitroazobenzene (Disperse Orange 3) were purchased from Aldrich and were used without further purification. Methacryloyl chloride was purchased from Fluka and was distilled before use.

4-(*N*-ethyl-*N*-(2-hydroxyethyl)amino)-4'-(4-nitrophenylazo)azobenzene

(3R). Disperse Orange 3 [4.8 g (0.020 mol)], 10 ml concentrated hydrochloric acid and 25 ml acetic acid were placed in a 100 ml beaker and cooled down in an ice-water bath. Sodium nitrite (1.4 g) in 8 ml water (kept in an ice-water bath) was then added dropwise to the above solution with stirring. The mixture was stirred at 0–5°C for 1 h. Added slowly to the mixture was 4 g (0.024 mol) of *N*-ethyl-*N*-(2-hydroxyethyl) aniline in 25 ml acetic acid while the temperature was kept below 5°C. After stirring for 10 h a large amount of a dark precipitate formed. The precipitate was collected by filtration and then washed with saturated sodium bicarbonate solution. The product was then dissolved in THF and passed through a silica gel column with a mixture of acetone and toluene as eluent. The second fraction (purple) was collected. Purple crystals were obtained after the solvent was rotoevaporated, mp 171°C. ¹H n.m.r. (DMSO-*d*₆): δ 1.15 (*t*, 3H, -CH₃), 3.45–3.65 (*m*, 6H, -CH₂-), 4.82 (*t*, 1H, HO-), 6.88 (*d*, 2H, aromatic, *ortho* to the N), 7.80 (*d*, 2H, on the benzene ring with amino group, *ortho* to -N=N-), 7.95 (*d*, 4H, on the benzene ring in the middle), 8.15 (*d*, 2H, on the benzene ring with nitro group, *ortho* to -N=N-), 8.45 (*d*, 2H, aromatic, *ortho* to NO₂).

4-[[2-[(2-Methyl-1-oxo-2-propenyl)oxy]ethyl]ethylamino]-4'-(4-nitrophenylazo)azobenzene

(3RM). 3R [2 g (0.0048 mol)] and 7 ml triethylamine (0.05 mol) were dissolved in 700 ml anhydrous THF. The purple solution was placed in an ice-water bath for 30 min and then 2.4 ml (0.024 mol) of methacryloyl chloride in 20 ml THF was added slowly dropwise while stirring. The mixture was allowed to warm up to room temperature after addition and was stirred at room temperature overnight. The solvent was rotoevaporated and the solid residue washed with saturated sodium carbonate solution followed by washing with water until the washing became neutral. Purple crystals (1.8 g) were obtained after recrystallizing the crude product from THF, mp 198°C. This compound has been previously reported but no characterization details were given^{7–10,15}. ¹H n.m.r. (DMSO-*d*₆): δ 1.15 (*t*, 3H, -CH₂CH₃), 1.83 (*s*, 3H, H₂C=C(CH₃)CO₂-), 3.55 (*m*, 2H, -NCH₂CH₃), 3.76 (*t*, 2H, -NCH₂CH₂O-), 4.30 (*t*, 2H, -CH₂O-), 5.68 (*s*, 1H, H₂C=C(CH₃)CO₂-, *cis* to -CH₃), 6.02 (*s*, 1H, H₂C=C(CH₃)CO₂-, *trans* to -CH₃), 6.95 (*d*, 2H, aromatic, *ortho* to the N), 7.82 (*d*, 2H, on the benzene ring with

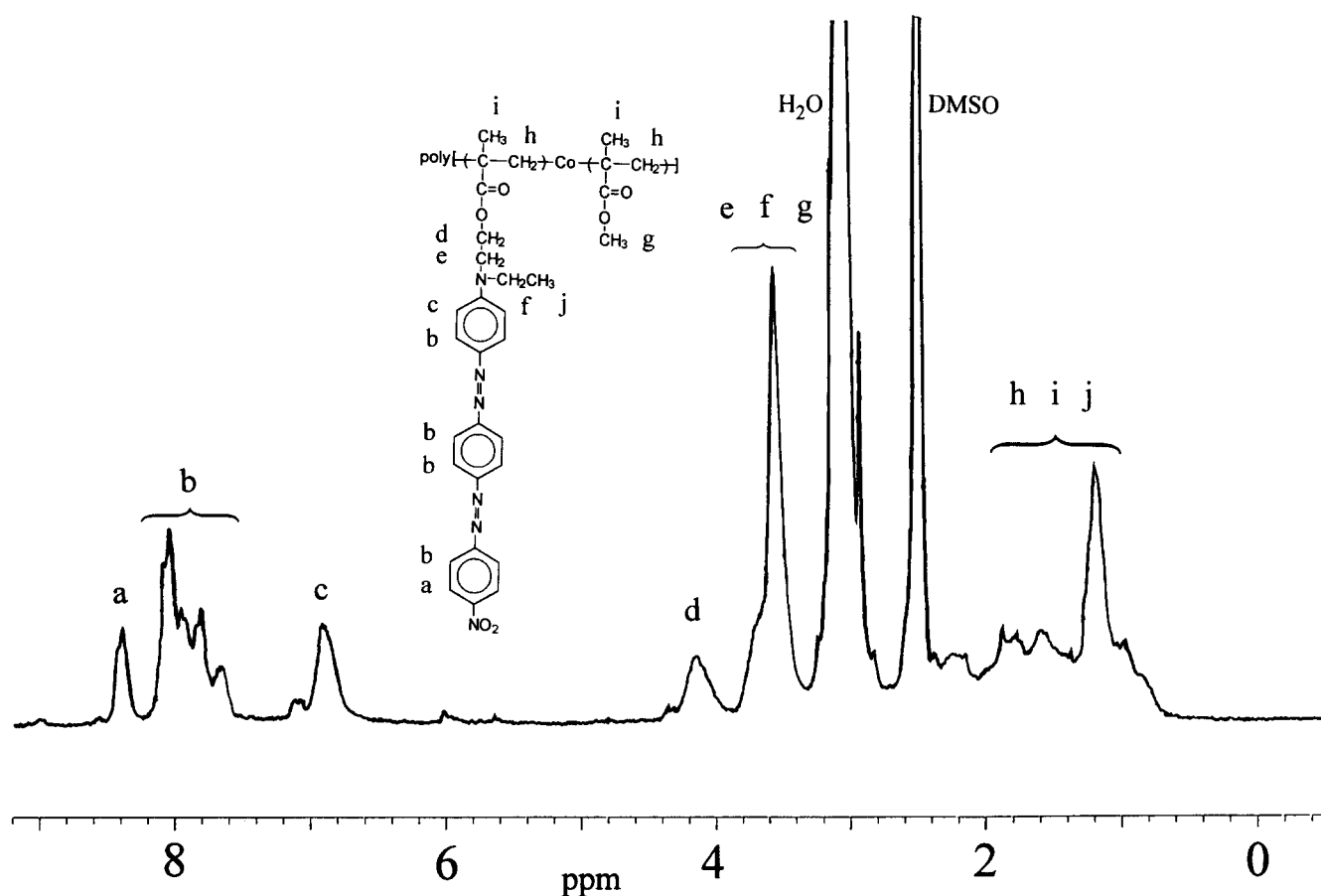


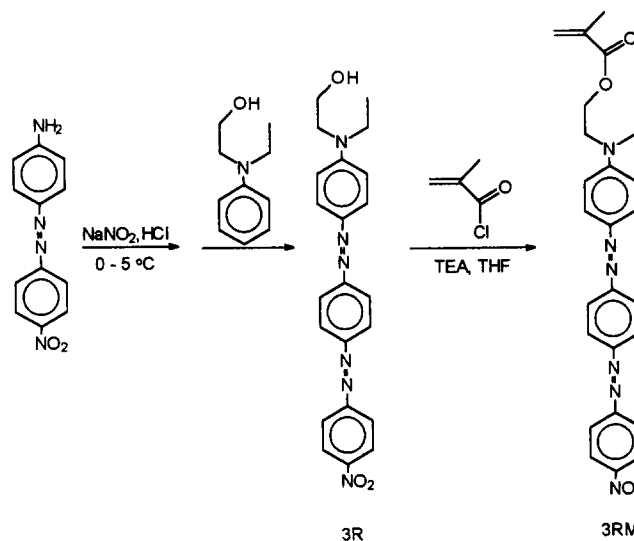
Figure 1 ^1H n.m.r. spectrum of poly(3RM-co-MMA), P3RMM30, in $\text{DMSO-}d_6$ at room temperature. The assignments are given on the spectrum

amino group, *ortho* to $-\text{N}=\text{N}-$), 7.98 (*d*, 2H, on the benzene ring with nitro group, *ortho* to $-\text{N}=\text{N}-$), 8.12 (*d*, 4H, on the benzene ring in the middle), 8.45 (*d*, 2H, aromatic, *ortho* to NO_2).

Polymerization procedure

The homopolymerization of 3RM and a few copolymerizations with methyl methacrylate (MMA) were carried out in 1,4-dioxane solution initiated with AIBN at 60°C . The homopolymer of 3RM is not soluble in common solvents such as THF, DMF, DMSO, toluene or chloroform. It is slightly soluble in nitrobenzene. The copolymers of 3RM with MMA were purified by several reprecipitations from THF/methanol until there was no monomer left in the product. The copolymer was then dried in vacuum at 50°C overnight. One sample with 11.6 mol% 3RM has a molecular weight of 6400. A ^1H n.m.r. spectrum of poly(3RM-co-MMA) is shown in Figure 1.

The films were prepared by spin-coating from the THF solutions onto glass substrates and dried in vacuum at 100°C for 20 h. The film thickness was 100–200 nm measured by interferometry. The procedure for reversibly inducing birefringence with a laser beam on the polymer film was described previously³. Writing and erasing were performed using an argon laser (514 nm) of 4.6 mW intensity on a spot of 1 mm in diameter at room temperature. Thermal transitions were measured on a Mettler TA-30 DSC instrument equipped with a TA-3000 processor at the scan rate of $20^\circ\text{C min}^{-1}$. Electronic spectra were recorded on a Shimadzu spectrometer. The molecular weights of the polymers were estimated by gel permeation chromatography (g.p.c.) on a Waters



Scheme 2

Associates liquid chromatograph equipped with a Model R401 differential refractometer and Model 440 absorbance detector. THF was used as the eluent. The solution ^1H n.m.r. spectra were obtained on a Bruker AC-F 200 n.m.r. spectrometer.

RESULTS AND DISCUSSION

The polymers

Scheme 2 gives the synthesis route for the monomer

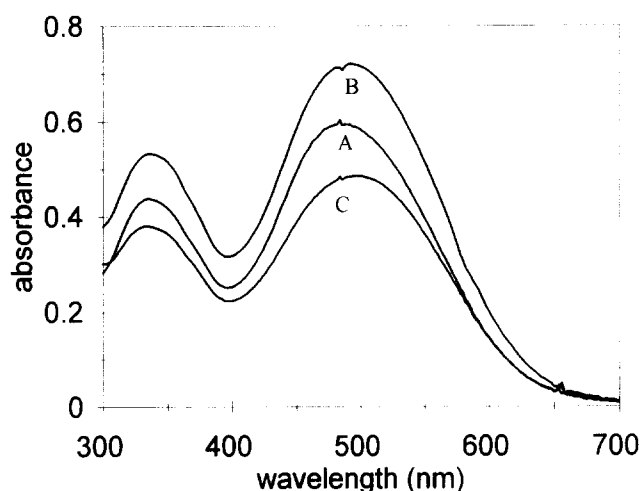


Figure 2 Electronic spectrum of poly(3RM-*co*-MMA) film with polarized light. Sample: P3RMM11 of 170 nm thickness for the film as cast (A), and the film after being subjected to polarized laser light recorded perpendicular (B) and parallel (C) to the polarization direction

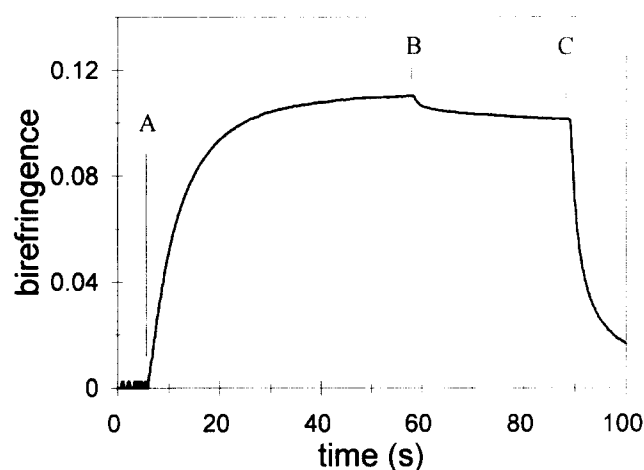


Figure 3 Writing-erasing curve of poly(3RM-*co*-MMA) film, sample: P3RMM11. At point A the linearly polarized laser (writing beam) is turned on; at point B the writing beam is turned off; at point C the circularly polarized laser (erasing beam) is turned on

3RM. We were unable to make a film of poly(3RM) because of its poor solubility in common solvents. Copolymerizing 3RM with MMA at different monomer ratios gave copolymers soluble in THF. Two copolymers, P3RMM11 (with 11.6 mol% 3RM) and P3RMM30 (with 30.0 mol% 3RM), were used in this study. The compositions of copolymers were obtained from ^1H n.m.r. spectra, an example shown in *Figure 1* for P3RMM30. The copolymer composition is calculated from the ratio of aromatic and methoxy peaks areas.

Poly(3RM-*co*-MMA) films exhibit a maximum absorbance (λ_{max}) at 490 nm shown as curve A in *Figure 2*. The occurrence of λ_{max} at longer wavelength for poly(3RM-*co*-MMA) in comparison with poly{4-[(2-(acryloyloxy)ethyl)ethylamino]-4-nitroazobenzene-*co*-MMA} (poly(DR1A-*co*-MMA)) of a similar MMA content¹⁶ is due to the larger conjugated system of the 3RM unit, which delocalizes the π electron and reduces the π - π^* transition (from -N=N-) energy. It also can be seen in *Figure 2* that the other absorption peak assigned to the π - π^* transition (from the benzene ring) in the u.v.

region appears at longer wavelength (about 330 nm) in comparison with the DR1A copolymer (about 280 nm). This has an effect of photoisomerization, and hence on the photoinduced birefringence. Poly(3RM-*co*-MMA) films are amorphous as proven by polarized microscopy and d.s.c. The d.s.c. curve of P3RMM11 shows a glass transition temperature at 113°C.

Structural factors affecting the photoinduced birefringence

A typical writing-erasing curve for a poly(3RM-*co*-MMA) is obtained when subjecting a polymer film to illumination with a 514 nm writing-erasing laser beam and using a 674 nm reading laser beam at room temperature. Such a curve for a P3RMM11 film is shown in *Figure 3*. The linearly polarized laser beam is turned on at point A and the birefringence is rapidly induced and reaches a saturated level. The birefringence relaxes at point B, where the writing beam is turned off, and reaches a stable level around point C. The induced birefringence is then completely eliminated by turning on the same laser, but circularly polarized, at point C, and the film is ready to be rewritten in the same manner. The saturated value of the photoinduced birefringence is about 0.11 and 0.13 for P3RMM11 (38.9 wt% azo monomer unit) and P3RMM30 (67.5 wt% azo monomer unit), respectively, which are much higher than the maximum birefringence achieved in poly(DR1A-*co*-MMA) with the same content (weight percent) of azo monomer unit (~ 0.05 and ~ 0.06 , respectively)¹⁶. This enhancement in birefringence can be explained by a combination of two factors:

(i) *The high length/width ratio of the 3RM structural unit.* Birefringence is defined as the difference in refractive indexes as follows

$$\Delta n = n_{\parallel} - n_{\perp} \quad (1)$$

where Δn is the birefringence and n_{\parallel} and n_{\perp} are the apparent refractive indexes parallel and perpendicular to the direction of the orientation (perpendicular to the writing direction). The values of n_{\parallel} and n_{\perp} reflect the polarizability of the molecular structure in the corresponding directions. As found in some liquid crystal polymer film doped with rod-like azo chromophores of different shapes, the higher the length/diameter ratios of the chromophore is, the higher the order parameter (as well as birefringence) will be¹²⁻¹⁴. As shown in *Scheme 1*, the azo chromophores in DR1A and 3RM have the same diameter, but 3RM has a longer conjugated system along the chromophore axis than DR1A. The large conjugated system yields a higher length-diameter ratio in 3RM in comparison with DR1A. It thus appears reasonable that poly(3RM-*co*-MMA) generates a larger birefringence value per chromophore than poly(DR1A-*co*-MMA) does.

To confirm the larger contribution to the birefringence of 3RM in comparison with DR1A, the photoinduced birefringence per azo chromophore was calculated by dividing the birefringence with the side group chromophore number density in the film. The birefringence per side group chromophore is 1.9×10^{-22} and 1.2×10^{-22} in P3RMM11 and P3RMM30, respectively. These values are almost one order of magnitude larger than those¹⁶ found in poly(DR1A-*co*-MMA) for the same azo weight contents, respectively; both are about 4×10^{-23} . The

higher birefringence per side group chromophore is probably the major reason for the higher birefringence induced in poly(3RM-co-MMA) films.

The polarized electronic spectra of poly(3RM-co-MMA) film show the difference in absorbance in the directions perpendicular to the writing direction (B in Figure 2) and parallel to the writing direction (C in Figure 2). The spectrum A in Figure 2 is the spectrum of an isotropic film. The dichroism is present in both the u.v. and visible regions. There appears to be no significant shape differences between the three spectra, indicating that the source of dichroism is mostly the reorientation of the *trans/trans* azo molecule. The birefringence, $\Delta n(\omega)$, at 674 nm can be calculated using the Kramers-Kronig transformation^{17,18}.

$$\Delta n(\omega) = \frac{c}{\pi} P \int_0^{\infty} \frac{\Delta \alpha(\omega')}{\omega'^2 - \omega^2} d\omega' \quad (2)$$

where $\Delta \alpha(\omega')$ is the dichroism, P is the principal value of the integral, ω is the measurement frequency, c is the speed of light, and ω' represents the whole spectrum. The calculated birefringence for P3RMM11 is 0.10 while the measured birefringence is 0.11. It is clear that both the u.v. and the visible regions contribute to the overall birefringence and this is different from poly(DR1A)¹⁷.

(ii) *Steric hindrances in photoisomerization and thermal randomization.* Two azo bonds have to photoisomerize in order to produce any motion of the chromophore with respect to its initial orientation. If just one of the azo bonds is photoisomerized to its *cis* configuration, the probability of returning to a *trans* configuration in the same position is overwhelmingly high. Thus, while the illumination is on, the process of orientation perpendicular to the light polarization should be much slower, since it should require many more cycles of *trans-cis-trans* photoisomerization. However, as the illumination is terminated after a certain saturation state is achieved, it should be equally difficult to achieve randomization, based on the fact that—again—two thermal *cis-trans* isomerizations should be taking place within the same molecule in order to move the 3RM structural unit. These 3RM structural units are more difficult to move around from a random to an organized distribution and more difficult to move from an oriented state to a random distribution.

The saturated level of birefringence is the result of a combination of two processes: photoselection, which increases birefringence, and thermal randomization, which decreases its level. These two processes reach an equilibrium state while illumination is on, and the preponderance of one or the other is determining the saturated level¹. The birefringence level is lower when the possibility for the azo chromophore to move around is great, for example in amorphous polymers doped with various azo chromophores. It is also known that the laser-induced birefringence in a poly(DR1A) film dramatically drops when the operating temperature increases¹. The 3RM copolymer films show a higher birefringence level in comparison with copolymers of DR1A having the same azo weight content, which reflects the decreased mobility of the chromophore containing the two azo bonds in comparison to the chromophore containing only one azo bond.

Table 1 Birefringence growth rates and normalized constants for equation (3)

	P3RMM11	P3RMM30	Poly(DR1A)
k_a (s ⁻¹)	0.21 ± 0.02	0.12 ± 0.02	4.1 ± 0.1
k_b (s ⁻¹)	0.08 ± 0.01	0.021 ± 0.002	0.22 ± 0.03
A_n^a	0.62 ± 0.02	0.68 ± 0.02	0.85 ± 0.01
B_n^a	0.38 ± 0.02	0.32 ± 0.02	0.15 ± 0.01
Correl. coeff.	0.99	0.99	0.99

$$^a A_n = A/(A + B); B_n = B/(A + B)$$

Another factor that has to be considered is the *dipolar interaction between the 3RM groups*. The neighbouring dipoles in the side chain of an azo polymer are oriented preferentially antiparallel to each other and the electric field of the neighbouring dipoles reduces the mobility of the azo groups¹⁶. This neighbouring dipolar effect depends on the azo content of the copolymer and is more significant when more dipoles are present (i.e. at higher azo concentrations). The birefringence per azo chromophore induced in P3RMM30 film is lower than in P3RMM11, but the total birefringence of P3RMM30 film is higher. The fact that there is a higher probability of dipolar interaction in P3RMM30 than in P3RMM11 (given by the number of the available dipoles) probably plays a role in this increase of the saturated level of birefringence.

Birefringence growth and relaxation rates

A biexponential curve fitting was used for birefringence growth [points A to B in Figure 3, equation (3)] and birefringence relaxation [points B to C in Figure 3, equation (4)] as follows^{5,6}:

$$\Delta n = A\{1 - \exp(-k_a t)\} + B \cdot \{1 - \exp(-k_b t)\} \quad (3)$$

where Δn represents the birefringence achieved at time t , k_a and k_b are the time constants for birefringence growth, and A and B are constants. The sum of A and B represents the maximum induced birefringence, and the normalized A ($A_n = A/(A + B)$), and B ($B_n = B/(A + B)$) represent the contribution of each of the two terms to the induced birefringence. The fitting parameters for birefringence growth are listed with the corresponding saturation birefringence levels in Table 1. The two processes are generally associated with photoisomerization and motion of the azo groups (the fast process) and with coupled motions of the side groups and the main chain (the slow process)^{5,6}.

$$\Delta n_r = C \exp(-k_c t) + D \exp(-k_d t) + E \quad (4)$$

In equation (4) Δn_r is the relaxed birefringence at time t after turning off the writing laser, k_c and k_d represent the time constants of the birefringence relaxation for the two kinds of motion (assigned as above—the fast one is related to the thermal *cis-trans* isomerization and various motions of the azo groups, and the slow one is related to coupled motions of the azo groups and the main chain), C and D are the constants related to the contribution of the two motions to the birefringence relaxation and E is the final birefringence independent of time. The sum of normalized C and D (C_n and D_n , respectively) describes the fraction of birefringence lost and the normalized E (E_n) represents the fraction of infinitely stable birefringence. The birefringence relaxation curve fitting results are listed in Table 2. These results are compared with those for poly(DR1A)

Table 2 Relaxation rates and normalized constants for equation (4)

	P3RMM11	P3RMM30	Poly(DR1A)
k_c (s ⁻¹)	0.94 ± 0.08	0.41 ± 0.01	1.5 ± 0.2
k_d (s ⁻¹)	0.044 ± 0.005	0.003 ± 0.001	0.07 ± 0.01
C_n^a	0.037 ± 0.003	0.014 ± 0.002	0.11 ± 0.01
D_n^a	0.056 ± 0.005	0.025 ± 0.005	0.11 ± 0.01
E_n^a	0.91 ± 0.01	0.96 ± 0.01	0.78 ± 0.01
Correl. coeff.	0.99	0.97	0.99

$$^a C_n = C/(C + D + E); D_n = D/(C + D + E); E_n = E/(C + D + E)$$

obtained in similar conditions. The fitting parameters for poly(DR1A) are also listed in *Tables 1* and *2*.

The writing rate constants for poly(3RM-co-MMA) in *Table 1* are smaller than poly(DR1A). Both k_a and k_b for the 3RM copolymers are more than one order of magnitude smaller than the same parameters for poly(DR1A). This is related to the larger size of 3RM, requiring more free volume in order to align in a certain direction, but—more importantly—the requirement of concordant photoisomerization of the two azo bonds in the same structural units (discussed above) means that more *trans-cis-trans* cycles are necessary in order to provide the same kind of side group mobility. This means that the whole process will take longer when 3RM groups are involved, as shown by the time constants. It is also interesting that the contribution of the slow process (B_n) in poly(3RM-co-MMA) is more significant than in poly(DR1A). This suggests that coupled motions between the side groups and the main chain are more important when the side group is larger.

Also, as discussed previously and as expected, the stability of the induced birefringence for poly(3RM-co-MMA) is higher than for poly(DR1A) (E_n in *Table 2*). P3RMM30 shows the highest E_n reported in amorphous polymers from this laboratory and elsewhere. It is also clear that the birefringence relaxation rates of poly(3RM-co-MMA) are lower than those of poly(DR1A). All of these can be attributed to the lesser mobility of the large conjugated azo side group.

CONCLUSIONS

Copolymers with side chains containing two azo bonds in one chromophore exhibit an enhancement in both photoinduced birefringence level and the stability in comparison to similar homo- and copolymers containing

just one azo bond. The high length/width ratio of the chromophore and the steric effects of the side chain motion are given as an explanation for the high birefringence level. The lesser mobility of the side chain groups produces the good stability of the induced orientation. This system would be ideal as a material for photonics, except that its very limited solubility severely restricts its potential utilization.

ACKNOWLEDGEMENTS

We thank the Office of Naval Research (U.S.), NSERC Canada and the Department of National Defence Canada for funding. A.N. thanks Canada Council for a Killam Research Fellowship.

REFERENCES

- Meng, X., Natansohn, A. and Rochon, P., *J. Polym. Sci., Part B: Polym. Phys. Ed.*, 1996, **34**, 1461.
- Natansohn, A., Xie, S. and Rochon, P., *Macromolecules*, 1992, **25**, 5531.
- Natansohn, A., Rochon, P., Gosselin, J. and Xie, S., *Macromolecules*, 1992, **25**, 2268.
- Natansohn, A., Rochon, P., Pézolet, M., Audet, P., Brown, D. and To, S., *Macromolecules*, 1994, **27**, 2580.
- Ho, M. S., Natansohn, A. and Rochon, P., *Macromolecules*, 1995, **28**, 6124.
- Ho, M. S., Natansohn, A., Barrett, C. and Rochon, P., *Can. J. Chem.*, 1995, **73**, 1773.
- Jones, F. and Reeve, T. J., *Mol. Cryst. Liq. Cryst.*, 1980, **60**, 99.
- Amato, M., Kaino, T. and Matsumoto, S., *Chem. Phys. Lett.*, 1990, **170**, 515.
- Kaino, T. and Tomaru, S., *Adv. Mater.*, 1992, **4**, 172.
- Buckley, A., *Adv. Mater.*, 1992, **4**, 153.
- Ahlheim, M. and Lehr, F., *Macromol. Chem. Phys.*, 1995, **196**, 243.
- Seki, H., Shishido, C., Yasui, S. and Uchida, T., *Jap. J. Appl. Phys.*, 1982, **21**, 191.
- Seki, H., Uchida, T. and Shibata, Y., *Mol. Cryst. Liq. Cryst.*, 1986, **138**, 349.
- Lackner, A. M., Sherman, E., Wong, S. Y. and Wong, S. M., *Mol. Cryst. Liq. Cryst.*, 1993, **14**, 763.
- Eckl, M., Müller, H., Strohmriegel, P., Beckmann, S., Eitzbach, K. H., Eich, M. and Vydra, J., *Macromol. Chem. Phys.*, 1995, **196**, 315.
- Brown, D., Natansohn, A. and Rochon, P., *Macromolecules*, 1995, **28**, 6116.
- Rochon, P., Bissonnette, D., Natansohn, A. and Xie, S., *Appl. Optics*, 1993, **32**, 7277.
- Nomura, S., Tobayashi, T., Nakanishi, H., Matsuda, H., Okada, S. and Tomiyama, H., *Proceedings of the SPIE*, Vol. 1560, 1991, p. 272.